Collision risk on final approach – a radar data based evaluation method to assess safety

ANP based Obstacle Assessment Surfaces

Christoph Thiel and Hartmut Fricke
Chair of Air Transport Technology and Logistic
Technische Universität Dresden, Germany
thiel@ifl.tu-dresden.de; fricke@ifl.tu-dresden.de

***Abstract*— Many major airports around the world are facing the problem of highly congested airspace and are therefore seeking ways to enhance capacity. Innovative RNP/ RNAV procedures in terminal areas, in particular RNP/ RNAV procedures for the final approach segment may be a possible solution due to increased flexibility when using the available airspace. However, these procedures must be designed according to their navigational performance requirements to ensure safe operations. Measuring safety of upcoming RNAV approach procedures in terms of navigational accuracy is crucial for their implementation at airports, as there is a need to develop specific obstacle assessment surfaces (OAS) and collision risk models (CRM). Designing specific OAS is essential for future airport development if benefits of improved navigational performance shall be fully exploited. This paper presents a method to determine actual navigational performance (ANP) during the final approach phase and a strategy for calculating ANP- based OAS executed here for an ILS final approach by means of radar data evaluation. Radar data will be used for statistical analysis of approach path deviations during the final approach phase and for modeling specific OAS based on the derived deviations.**

Safety; Collision probalility; Actual navigation performance (ANP); Obstacle Assessment Surfaces; Radar data analysis

I. INTRODUCTION

The objectives of the *SESAR* ATM Master Plan [1] are amongst others to enhance the capacity of the European air traffic system by a factor of three and at the same time enhance safety by a factor of 10. To reach these ambitious goals, new flight procedures need to be developed and implemented, especially at already nowadays highly congested terminal areas (TMA) around major European airports. Take off and landing, which take place here, are still the most critical flight phases, as the majority of all accidents (56% of all fatal accidents) occur during these phases, although they only cover about 6 % of the total flight time for a typical 1.5 hour flight. When only considering final approach and landing, the ratio is at 4 % flight time to 36 % of fatal accident likelihood [2].

So the flight phases take off and landing are preferred fields to improve safety in the European air traffic system. Improvements may be reached by introducing new approach procedures such as RNP/RNAV approaches, requiring a navigational accuracy during final approach (non-precision) of at least 0.3 NM. In detail, this expresses a Required Navigation Performance (RNP) of 0.3 NM cross and along the desired flight track for 95% of the flight time. This equals the two sigma interval of a normal distribution. RNAV approaches may increase safety, which could not be analytically demonstrated until now, but doubtlessly it will improve capacity of airports, especially in obstacle rich environments, as the lateral and vertical approach path is more flexible to adapt to environmental requirements.

However, measuring safety in terms of navigational accuracy of upcoming RNAV approach procedures is crucial for their implementation at airports, as e.g. there is a need to develop specific obstacle assessment surfaces (OAS) and collision risk models (CRM) for these kind of procedures according to ICAO airspace design requirements. Along those, ICAO PANS-OPS [3] methods to construct OAS and apply CRM are described already for e.g. innovative GBAS CAT I approach procedures. However, they are not specifically explored - they simply use the same OAS and CRM calculation method as for the reference ILS CAT I approach, with only few adjustments for OAS constants.

This paper presents a method to determine the navigational accuracy (actual navigation performance – ANP) which shall always be higher than the design RNP value. We focus on the final approach segment based on a radar data analysis taken from live traffic in 2008. Due to the lack of radar data of an innovative RNAV approach procedure, the analysis is based on an ILS final approach segment. Nevertheless, the described method can be fully adopted for RNAV final approach procedures when such data will become available, although results may be different from those shown here, due to different navigational performance. Knowing navigational accuracy of specific flight segments is essential to estimate collision risks [4], [5] and to derive obstacle assessment surfaces for a specific procedure. Therefore finally a method will be shown, how to construct OAS using determined ANP for the investigated procedure.

II. NAVIGATIONAL ERRORS

Collision risk during final approach firstly depends on the relative position of an object (obstacle) to the nominal approach path and secondly on the navigational accuracy of

approaching aircrafts, so their along and cross track tolerance. The following section will give a systematic overview of navigational errors during final approach depending on the flown procedure.

A. Navigational errors during conventional approach procedures

The navigational accuracy during conventional approach procedures, of which the ILS approach is the most important one, is influenced by the following three error categories:

- Errors of ILS ground equipment – LLZ and GP antenna signals (GEE, ground equipment error),
- Errors of airborne equipment – LLZ and GP receiver and indicator (AEE, airborne equipment error) and
- The difference between desired and true trajectory – errors induced by the pilot/ autopilot (FTE, flight technical error)

The Total System Error (TSE) is denoted as the root sum square of these three categories:

$$TSE = \sqrt{GEE^2 + AEE^2 + FTE^2}$$

B. Navigational error of RNP-RNAV procedures

The inability to achieve the required navigation performance during RNAV procedures may be due to navigation errors related to aircraft tracking and positioning in the context of on-board performance monitoring and alerting as it is mandatory for RNAV procedures. According to ICAO Manual on Performance Based Navigation (PBN) [6] the navigational errors for RNAV contain the following three main error categories:

- Path definition error (PDE)
- Flight technical error (FTE) and
- Navigation system error (NSE)

The PDE occurs when the path defined in the RNAV system database does not correspond with the desired path. Flight Technical Errors are again errors induced by the pilot/autopilot including display errors. The NSE refers to the difference between the aircraft's estimated position and actual position. So this is the error of the multi-sensor navigation system, as e.g. the error of the GPS. The TSE is again the root sum square of three error categories, here PDE, FTE and NSE.

C. Accuracy requirements for current RNAV approach procedures

The ICAO PBN Manual [6] defines two types of RNAV approach procedures which are applicable to the final approach segment. First, the "non precision alike" RNP APCH which is defined as an RNP approach procedure that requires a lateral TSE (Along Track and Cross Track) of ±1 NM in the initial, intermediate and missed approach segments and a lateral TSE of ±0.3 NM in the final approach segment. Second, the RNP AR APCH (authorization required), which is defined as RNP approach procedure requiring a lateral TSE of at least ±0.3 NM and down to ±0.1 NM for all approach segments.

D. Accuracy requirements of upcoming RNAV approach procedures

With the application of RNP concepts to approach procedures, and in particular to upcoming precision approaches, the All Weather Operations Panel (AWOP) had concern in also addressing a required vertical navigational accuracy beside along and cross track tolerances. As a result, a range of RNP types were defined from RNP 0.3 down to RNP 0.003/z, where z reflects the requirement for vertical guidance. The following Tab. I collects all proposed RNP types with vertical and lateral TSE according to [7]:

TABLE I. PROPOSED RNP TYPES FOR FINAL APPROACH SEGMENTS [7]

RNP Type	Required Accuracy (95% containment)	Description
0.003/z	± 0.003 NM [± z ft]	Planned for CAT III Precision Approach and Landing including touchdown, landing roll and take-off roll requirements. (ILS, MLS and GBAS)
0.01/15	± 0.01 NM [± 15 ft]	Proposed for CAT II Precision Approach to 100 ft DH (ILS, MLS and GBAS)
0.02/40	± 0.02 NM [± 40 ft]	Proposed for CAT I Precision Approach to 200 ft DH (ILS, MLS and GBAS)
0.03/50	± 0.03 NM [± 50 ft]	Proposed for RNAV/VNAV Approaches using SBAS or GBAS
0.3/125	± 0.3 NM [± 125 ft]	Proposed for RNAV/VNAV Approaches using Barometric inputs or SBAS inputs.

E. Errors of radar antenna system

Before applying the method to analyse the aircraft's ANP by means of radar data analysis one more additional error needs to be considered.

Although the TSE of the researched procedure (regardless of which) can be measured with the here applied radar data analysis, it should be noticed, that this measurement may be non-precise due to erroneous radar antenna system data itself. Due to angular signal characteristic of the radar system, the error will increase with increasing distance to the radar facility. The magnitude of this radar equipment error is not quantifiable right now, due to lack of adequate data. Nevertheless, when focussing on a specific, relative small investigation area, as it is performed here, the error for all covert data points will be within the same range and therefore will have only a small impact for the statistical analysis applied here. Consequently, it could be assumed, that due to this additional error all here shown results has to be considered as conservative results. The TSE during final approach may be effectively lower than the measured one by means of a radar data analysis.

III. DATA SOURCE

The radar data used for the analysis are taken from the Flight Track and Aircraft Noise Monitoring System (FANOMOS) of the German ANSP *Deutsche Flugsicherung GmbH* (DFS). These tracks compile all transponder equipped arrivals and departures at a major German airport for a period of six months (busiest six month – May to October). As these radar data are classified as confidential, the airport has to be treated anonymous and will be named as *investigation airport* in this paper. The recorded data comprehends the aircraft flight tracks in terms of single data points (position of aircraft, identification and aircraft reported altitude via SSR Mode A/C resp. S) recorded at an update rate of 4 sec and complemented by flight plan data. In detail, the following information are forming a data bloc:

- Flight plan data (e.g. date, aircraft type, call sign, used runway, time of arrival/ departure)
- Radar data:
    - Time stamp, measured in seconds from first recording
    - Horizontal positional information – X, Y coordinates in UTM WGS84 format
    - Vertical positional information –altitude in meter above mean sea level
    - Ground speed in meter per second
    - Distance in meter, measured from first recording

Altogether 81'084 flight movements were sampled at the investigation airport and recorded by FANOMOS in this half year time period in 2008. So, the recorded data consist of more the 8.3 million single data points at a resolution of 4 seconds. The data are given in tabular form in ASCII Format.

IV. STATISTICAL ANALYSIS OF APPROACH PATH DEVIATIONS DURING ILS FINAL APPROACH

A. *Methodological overview*

Based on the available radar data the deviation probability from the nominal flight path will be calculated, performing the following steps:

1. Selection of usable data (ILS approach only)
2. Definition of final approach segment and splitting into investigation segments (cross sections) along the approach path in fixed steps
3. Determination of lateral (cross to the flight path) and vertical deviations from final approach path at every cross section
4. Determination of mean and standard deviation in lateral and vertical direction
5. Modelling of approach path deviations as distributions related to the distance to the threshold
6. Verification of the resulting distribution functions.

B. *Selection of useable data*

As explained in the previous Chapter III, used radar data conclude all air traffic movements at the investigation airport within a time period of half a year. So, the first step in determining the approach path deviation is to select a specific number of flight tracks out of radar data base, which are doubtlessly precision approaches, as ILS final approach is focused procedure here. Therefore, the following steps were performed to filter the data base:

- Identify the flight phase: Either approach or departure
- Identify the landing direction
- Split precision and non precision approaches

After these steps, altogether 14'500 precision approach flight tracks were found for further statistical analysis. The following Fig. 1 shows an extract of these flight tracks (approx. 700 approaches are shown):

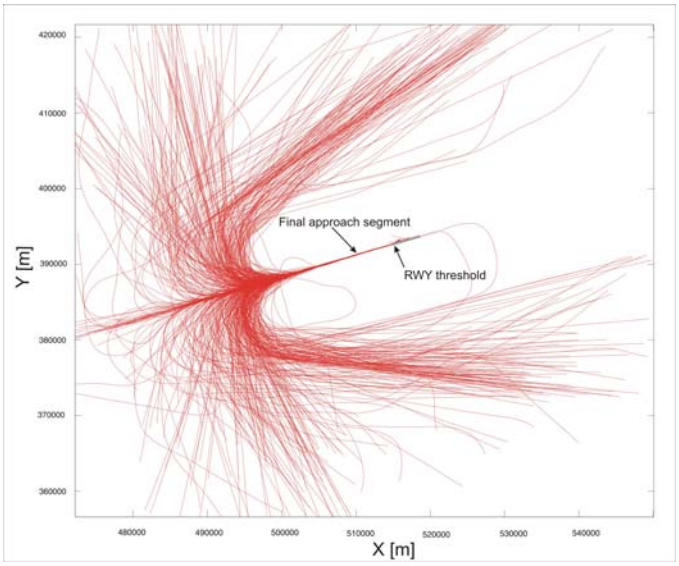

Figure 1. flight track snapshot – ILS approach

Already the visual comparison shows the much higher navigational performance during final approach than e.g. during the intermediate approach phase (concentration of flight tracks on the final approach segment) inline with the presented ICAO RNP/RNAV concept, as presented in Chapter II.

C. *Quantification of path deviations*

Starting from the landing threshold and following the approach path in the opposite direction, cross section windows were defined at 1000m distance intervals along the approach path ending at the final approach fix (typically located about 8 to 12 NM threshold distance).

Afterwards, the intersection points of the fight tracks at each defined cross section window were determined. This is based on linear interpolation between two radar data points from the flight track information (as update frequency of radar antenna is 0.25Hz distance between two data points ranging between about 150 m and 400 m depending on the final

approach speed). The lateral as well as vertical deviation (altitude deviation) from the nominal flight path was determined for all cross section windows. Subsequently all outliers were removed from the data base by the Grubbs-outlier test. Outliers are data points, which are significantly different from the all other data points. Such outliers could be caused by e.g. missed approaches or late LLZ or GP intercepts. Overall, only a few outliers (less than 0.5%) were identified and therefore removed.

The following Fig. 2 exemplarily represents the determined flight intersection points for the 6'000m cross section window (6'000 m threshold distance):

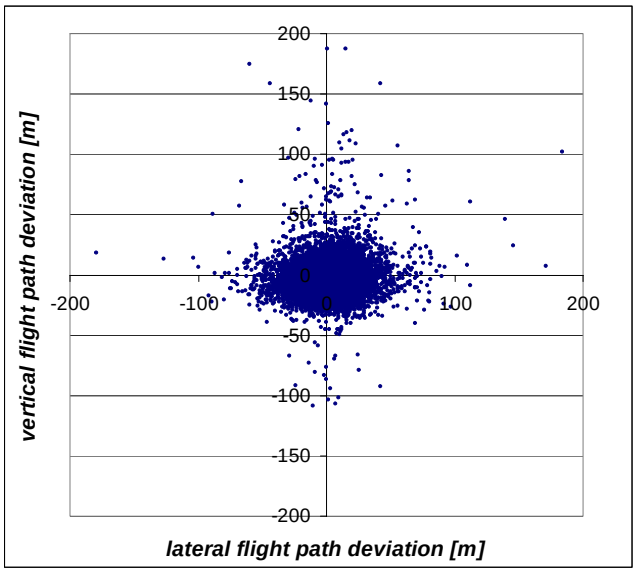

Figure 2. Measured Deviations from nominal track at 6000m distance to threshold

As expected, Fig. 2 shows a clear concentration around the nominal approach path: for the shown cross section window most of measured intersection points are deviating less than 50 m in lateral and less than 25 m in vertical direction. For comparison purposes: one dot deviation on the HSI/ PFD for ILS LLZ resp. GP equals to 83 m in lateral and 28 m in vertical direction for this threshold distance.

D. Quantification of underlying distribution function

Next step in determining the approach path deviations by modelling location probability functions (PDF) is to find a PDF that fits the measured deviations. Air traffic safety research at TU Dresden shows that a normal distribution function is most often best fit for describing navigational accuracy for many approach and departure procedures [8], [9]. Therefore a normal distributed behaviour will be assumed as underlying distribution. In order to check legitimacy of the assumption of a normal distribution, exemplary all available data of the 6000m section were statistically analyzed. To that purpose, the data will be arranged into classes of a specific number and range using statistical methods. The number of classes and the dimension of their range can be defined freely, but the number of classes should be in between five and about twenty. A common used approximation of the number of required classes is:

$$k \leq 5 \cdot \lg(N) \tag{1}$$

where N corresponds to the sample size (here number of given arrivals). Then the associated class range k_b is calculated from the bandwidth of the ascertainment data:

$$k_b \approx \frac{X_{\max} - X_{\min}}{k} \tag{2}$$

According to this calculation, a number of 21 classes is produced with a class range of 8 m for the lateral direction and respectively 21 classes with a class range of 6 m for the vertical direction. The following Fig. 3 shows exemplarily for the 6000m section, the class frequency according to the determined grading for the lateral as well as the vertical direction:

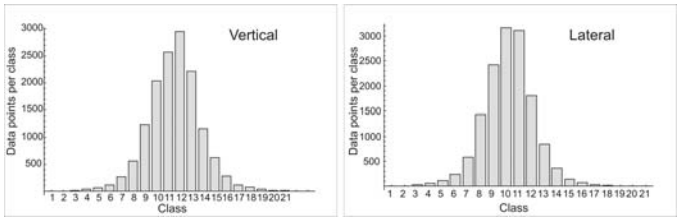

Figure 3. classified distribution in lateral and vertical direction at 6000m cross section window

Like Fig. 3 shows, the distributions seem to follow normal distributions in lateral as well as in vertical direction. The normal distribution is depending on the two parameters mean value μ and standard deviation σ, only. The one-dimensional density function of the normal distribution appears as follows:

$$f(x) = \frac{1}{\sigma\sqrt{2\pi}} \cdot e^{-\frac{(x-\mu)^2}{2\sigma^2}} \tag{3}$$

Now it is possible to determine the mean value as well as the standard deviation in lateral and vertical direction for all 13 cross section windows out of these data points. With assumption of a normal distribution, location probability functions can be calculated on the basis of these two statistical parameters.

For the cross section window, which is demonstrated exemplarily, the following mean was calculated for the lateral and vertical direction:

$$\mu_{lateral} = 1.34m \text{ and } \mu_{vertical} = 2.65m.$$

For the standard deviation follows:

$$\sigma_{lateral} = 16.25m \text{ and } \sigma_{vertical} = 11.36m.$$

The following Fig. 4 shows quantitatively the progresses of normal distribution functions determined as described for the lateral and vertical direction, compared to the class frequencies of the sample already illustrated in Fig. 3:

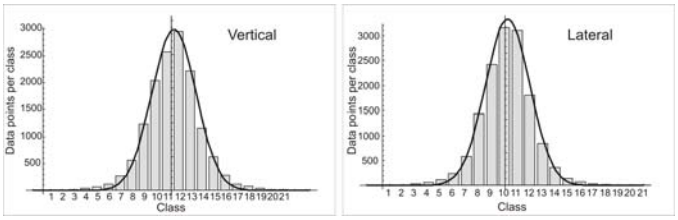

Figure 4. Distribution in lateral direction and approximated normal distribution, 6000m section

Fig. 4 shows explicitly that the progresses are following the normal distribution "very well". The statistical test using coefficient of determination and F-Test documents this objectively too, wherewith the legitimacy of the figure with the distribution of the approach accuracy in lateral and vertical direction is detected through a normal distribution. The Chi-Square-Test, which is also often used for such tests, is not applicable for such big sample sizes.

E. Determination of distribution parameters for all cross section windows

Now the determination of the distribution parameters mean and standard deviation are performed for all defined, previous cross section windows along the approach flight path. The following Tab. II represents determined values of standard deviation and mean value for each of the 13 sections in lateral and vertical direction:

TABLE II. DEVIATION PARAMETER DURING ILS APPROACH, ALL SECTIONS, VERTICAL AND LATERAL

Cross section window	threshold distance [m]	Lateral		Vertical	
		Mean [m]	Standard deviation [m]	Mean [m]	Standard deviation [m]
Section 0	0	1.357	9.283	1.236	8.828
Section 1	1000	12.917	12.652	1.265	8.878
Section 2	2000	26.654	16.025	1.690	8.431
Section 3	3000	32.632	18.074	2.779	9.115
Section 4	4000	28.339	17.295	3.653	9.641
Section 5	5000	15.240	16.255	3.569	10.408
Section 6	6000	1.342	16.247	2.649	11.360
Section 7	7000	-9.285	17.521	1.809	12.602
Section 8	8000	-15.575	20.292	1.825	14.026
Section 9	9000	-18.452	23.600	2.192	15.702
Section 10	10000	-20.028	27.542	1.461	17.775
Section 11	11000	-20.774	32.535	-1.234	20.085
Section 12	12000	-21.572	40.349	-5.354	22.313

As expected, Tab. II shows a distance-depending distribution characteristic relating to threshold distance: The greater the distance to the threshold, the greater is the distribution (standard deviation) in lateral as well as vertical direction. Furthermore, in lateral direction, a slightly oscillating behaviour around the nominal flight path could be observed. In vertical direction, for all sections (instead of far threshold distances) the mean value for vertical direction is above the flight path. It's assumed that many hand flown approaches are intentionally performed slightly above the glide slope for safety purposes.

Now, the distance dependency can be approximated via linear interpolation, wherewith it is possible to determine the given distributions for any threshold distance, analytically.

According to this, for lateral deviation applies the following distance dependency for the standard deviation linear fitted:

$$\sigma_{lateral}(x) = 0.002x + 8.86 \quad (4)$$

with x = threshold distance in [m] and σ(x) = lateral standard deviation in [m]. Thus the standard deviation amounts to 8.86m on threshold and is increasing about 2m per each 1000m distance to the threshold (respective 0.11°). Analogue, for the vertical deviation applies the following distance dependency for the standard deviation:

$$\sigma_{vertical}(x) = 0.00113x + 6.25 \quad (5)$$

Thus, the standard deviation amounts to 6.25m on the threshold and is increasing about 1.13m per each 1000m threshold distance (respective 0.065°). Both fits (lateral and vertical) are valid for a threshold distance up to 12'000 m. The acceptance was checked again via coefficient of determination and F-Test for both function approximations.

In conclusion, the assumed distance dependency of flight path deviations during ILS final approach – increasing lateral and vertical deviation with increasing threshold distance – could be shown with the presented statistical analysis.

F. Discussion of results

The given deviations can be converted into ANP values according to RNAV convention (95% or two sigma containment in NM) for comparison purposes. The following Tab. III represents ANP values in lateral (cross track tolerance – XTT) and vertical direction (vertical track tolerance – VTT) for some exemplary threshold distances:

TABLE III. EXEMPLARY ANP VALUES (XTT AND VTT) FOR ILS FINAL APPROACH

Distance to threshold	XTT	VTT
0 m	0.012 NM	0.008 NM
2500 m	0.015 NM	0.010 NM
5000 m	0.020 NM	0.013 NM
10000 m	0.031 NM	0.019 NM

As seen in Tab. III, XTT values range between 0.01 NM and 0.03 NM and VTT values between 0.01 and 0.02 NM. Compared with Tab. I, these values are in a range of about CAT I to CAT II approaches. RNP values for CAT III compliance are not reached, although the investigated airport is ILS CAT IIIb equipped. This is most likely due to the investigated time period during summer month. As CAT II/III conditions are very rare (at a guess less than 1% of all approaches are performed under CATII/ III conditions) most approaches were on a CAT I approach. Furthermore the above given XTT and VTT can now be compared with ICAO Annex 10 [10] requirements for ILS CAT I. The following Fig. 5 represents the comparison of the here determined lateral

deviations (XTT) with ICAO tolerances for localizer (LLZ) signals for an ILS CAT I approach, for both the (±) 95% containments are shown:

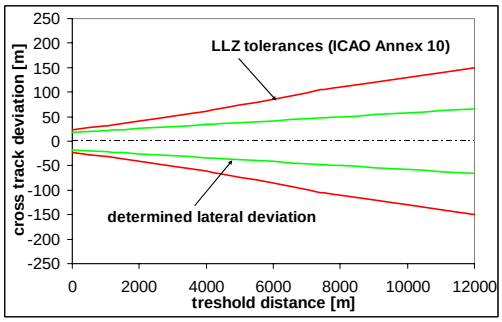

Figure 5. lateral deviations vs. ICAO tolerances for LLZ

Fig. 6 below represents the comparison of the previously determined vertical deviations (VTT) with ICAO Annex 10 tolerances for glide path (GP) signals. For both, the (±) two sigma intervals are shown:

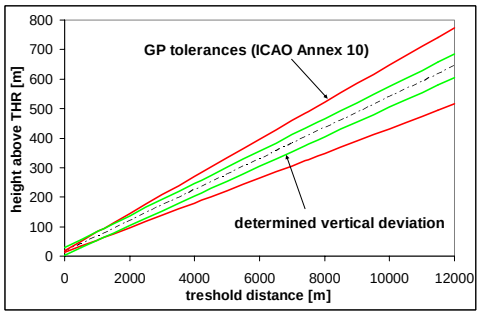

Figure 6. vertical deviations vs. ICAO tolerances for GS

As seen in Fig. 5 and Fig. 6 the derived lateral and vertical deviations are significantly below ICAO Annex 10 requirements, even though derived deviations are TSE and ICAO requirements need to be considered as just GEE, which is only one part of the TSE (see Chapter II). It's assumed that ICAO requirements were developed decades ago on basis of the achievable navigation performance of that time (e.g. ICAO collision risk model [11] was developed in the 70ies decade). But navigation performance is supposed to have significantly improved since then due to technical improvements on ground equipment as well as airborne equipment, which might be a reason for these findings. Higher vertical deviations very close to threshold (see Fig. 6 – less then app. 1000 m threshold distance) may be caused by radar equipment error, due to radar reflecting characteristics for ground near targets.

V. MODELLING OF ANP- BASED OBSTACLE ASSESSMENT SURFACES

A. *PANS-OPS OAS approach surfaces*

Obstacle assessment surfaces (OAS) according to PANS-OPS [3] are imaginary surfaces which guarantee obstacle free approach (in detail a collision risk below the Target Level of Safety of 1×10^{-7} per approach), when operating under instrument flight rules (IFR) on precision or non-precision instrument approach. The OAS system is based on collision risk calculation of ILS Collision Risk Model (CRM) [11]. For the CRM collision risk functions (normal distributed PDF's in vertical and lateral direction) the 1×10^{-7} per approach probability curve (contour of same collision risk during the precision segment of an ILS approach) is used for surface modelling. At this curve tangential surfaces in trapezoid shape were fitted, to get defined, plane surfaces which guarantee a collision risk less then 1×10^{-7} per approach. The following Fig. 7 shows the 1×10^{-7} per approach probability curve and the tangential placed surfaces, which form the OAS final approach funnel according to [12]:

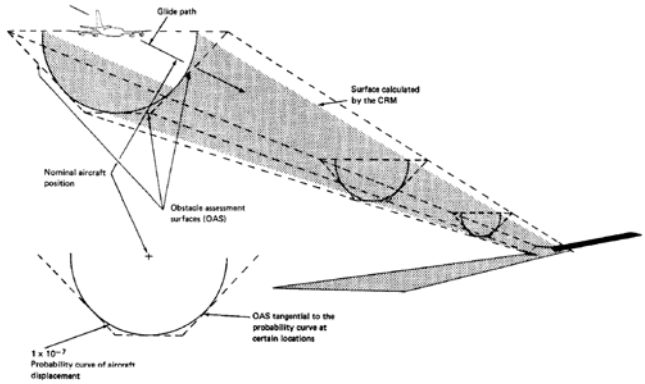

Figure 7. OAS approach funnel acording to [12]

As seen in Fig. 7, the approach surfaces are getting closer, the closer the distance to the landing threshold is, so this also shows the angular signal characteristic of the ILS.

B. *Potential shapes of ANP based OAS*

As seen in the previous chapter PANS OPS defines plane surfaces embedding the CRM 1×10^{-7} collision risk contour. The construction of such surfaces is per se not necessary, as the CRM contour already gives an area of maximum allowable collision risk, but in shape of tapering ellipses that are difficult to describe. Due to simplification matters for airport procedure designers this is approximated conservatively by the described tangential surfaces. But this simplification leads to an overestimation of collision risk in some specific areas, as the surfaces are bigger than the ellipses. By construction of other shapes than the trapezoid surfaces this overestimation could be decreased, but this is always associated with a more complex surface design. The following Fig. 8 shows some potential tangential surface shapes ordered from simple to complex:

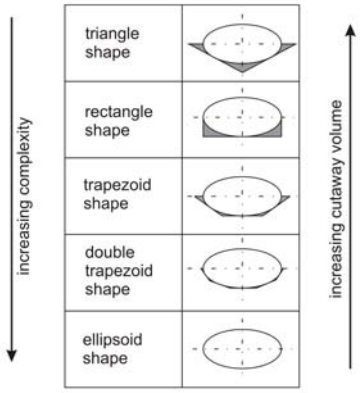

Figure 8. potential surface shapes

With increasing complexity the cutaway volume (volume between ellipse and tangential surfaces) will decrease significantly and additionally the overestimation of collision risk decreases. This cutaway volume can be expressed as overestimation volume in percent of the half-ellipsoid volume. This is for triangle and rectangle shape about 27.3%, for trapezoid shape about 10.3 %, for double trapezoid shape about 3.4% and for the ellipsoid shape 0%. So when only looking at cutaway volumes, the best solution appears to be the ellipsoid shape, but when taking design criteria into consideration this would be the most unpractical solution, as the more complex the shapes – the more complex is the calculation scheme, which makes it unsuitable for airport procedure designers.

So it could be assumed, that the trapezoid shape is the best compromise between complexity and risk overestimation. Therefore the following chapter will describe the method of shape modelling focussing on trapezoid shape.

C. Construction of radar- fitted approach surface

Based on the in Chapter IV shown deviation functions in lateral and vertical direction, we are now able to construct obstacle assessment surfaces for derived ANP during final approach. Firstly, we need to calculate the size of the 1×10^{-7} contour, in other words to calculate the $1\text{-}1\times10^{-7}$ quantile of the lateral and vertical PDF. Furthermore the maximum size of an approaching aircraft needs to be considered, here according to ICAO Annex 14 [13] a category F aircraft was considered, which is e.g. the Airbus A380 as current largest commercial aircraft. The semi-span (40 m) was added to the 1×10^{-7} contour of the lateral distribution function and the distance between the glide path antenna and the lowest point of the landing gear (8 m) was added to 1×10^{-7} contour of the vertical distribution function. The following Fig. 9 shows the general method of determination of the radar- fitted OAS approach surfaces exemplarily for 1'000 m threshold distance:

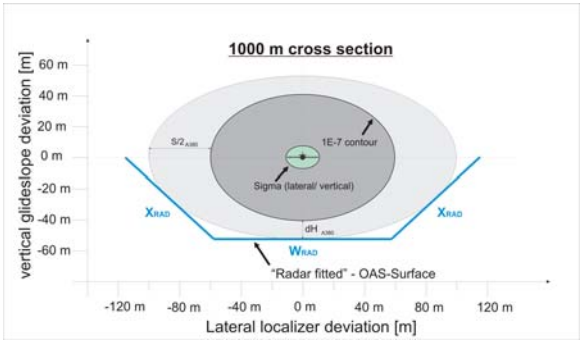

Figure 9. exemplary surface modelling for 1.000 m cross section

The inner (green) ellipse in Fig. 9 shows the dimension of the one sigma interval (standard deviation) for the 1000 m cross section window (see also Tab. II) centred on the nominal flight path. The surrounding darker gray ellipse shows the 1×10^{-7} per approach contour. Moreover, the surrounding light-grey ellipse takes the size of Cat F aircraft into consideration.

On the outer edges of this ellipse tangential surfaces in trapezoid shape (blue lines in Fig. 9) analogue to OAS approach surface were modelled. The tangential surfaces were constructed in such a way, that the volume between the surfaces and the outer ellipse was minimized, in order to have as less refuse as possible. When applying this method for every cross section window, a linear increasing approach funnel around the nominal approach path will be formed, due to the distance dependency of the modelled PDF's (increasing distribution with increasing threshold distance) and linearization of distribution parameters. A surface modelling above the nominal flight path is not necessary, as it is assumed that any path deviation above the glide slope signal is uncritical for obstacle assessment. The following Fig. 10 gives a top view of the assessed OAS:

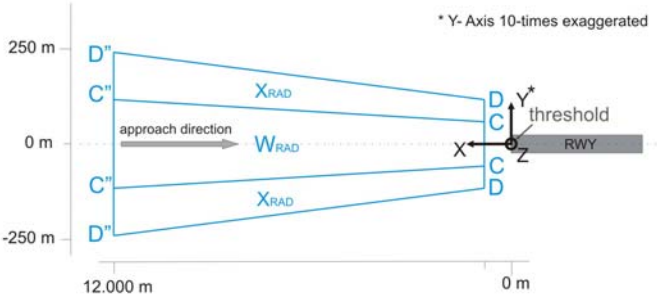

Figure 10. determined ANP- based OAS final approach surface – top view

The blue lines in Fig. 10 are marking the edges of OAS surfaces as determined. The corners on each side were named according to PANS-OPS declaration with the capital letters C and D for the threshold nearest corners and with C" and D" for the opposite corners. For clarification purposes, Tab. IV below summarizes the corner coordinates, were the origin of the coordinate system is located on the threshold (see also Fig. 10) with z=0 at threshold elevation:

TABLE IV. COORDINATES OF DETERMINED OAS SURFACES

Corner point	Corner Point Coordinates		
	X	Y	Z
C	543 m	+/- 52.93 m	0 m
D	543 m	+/- 105.94 m	43.69 m
C"	12'000 m	+/- 122.03 m	533.12 m
D"	12'000 m	+/- 243.18 m	644.13 m

As seen the determined OAS surfaces are not ending at the threshold (line D-C-C-D in Fig. 10). The threshold distance at the end of surfaces is 543 m, this is the point were the W-surface is at the same altitude as the landing threshold and therefore the ground collision risk reached the TLS. This can be seen as the obstacle clearance height (OCH) for an obstacle free environment (ground collision risk determines the OCH), which is about 44 m (143 ft) in this case.

VI. CONCLUSION

Design of specific Obstacle Assessment Surfaces for current and upcoming approach procedures is crucial for future airport development when benefits of improved navigational performance shall be fully exploited. This paper presented a method to determine navigational performance during the final approach phase and a strategy for calculating ANP- based OAS executed for ILS final approach. This method may easily be transferred to innovative RNP/RNAV approach procedures, when respective reference data becomes available. Nevertheless, the results of a statistical approach path deviation analysis for RNAV procedures may be different to the here shown results for ILS approach (see Fig. 10). Due to angular signal characteristics of ILS radio signals, an increasing approach funnel was found. Based on the non-angular characteristic of RNP/RNAV procedures this funnel is assumed to convert into a tube covering the entire final approach segment. Consequently, geometric advantages of this design concept appear with increasing threshold distance.

REFERENCES

[1] SESAR Consortium, "European Air Traffic Management Master Plan", Edition 1, 30.03.2009

[2] Boeing Commercial Airplane Group, "Statistical summary of commercial jet airplane accident, worldwide operations 1959 – 2008", Seattle, July 2009

[3] ICAO, "Procedures for Air Navigation Services – Aircraft Operations (PANS-OPS), Volume I, Doc. 8168", 5th Edition, Montreal, 2006

[4] H. Fricke, "Integrated collision risk modelling - CoRiM: An airborne safety and protection system for upcoming ATM concepts", ISBN 3-89574-418-2, Berlin, 2001

[5] M. Vogel, C. Thiel and H. Fricke: "A quantitative Safety Assessment Tool based on Aircraft Actual Navigation Performance", unpublished (to appear at ICRAT 2010)

[6] ICAO, "Performance-based Navigation (PBN) Manual, DOC 9613-AN/937", 3rd Edition, Montreal, 2008

[7] Eurocontrol, "Guidance Material for the Design of Terminal Procedures for Area Navigation (DME/DME, B-GNSS, Baro- VNAV & RNP-RNAV)", 3rd Edition, March 2003

[8] C. Thiel, „Untersuchung der Navigationsgenauigkeiten von Luftfahrzeugen im Flughafennahbereich - Modellierung und Implementierung dreidimensionaler Verteilungsfunktionen unter Berücksichtigung der Navigationsinfrastruktur an großen Verkehrsflughäfen", Diploma Thesis, TU Berlin, Berlin, June 2009

[9] M. Kietzmann and H. Fricke, „Entwicklung eines quantitativen Bewertungsmodells zur objektiven Beurteilung des Einflusses neuer Betriebsverfahren auf die Sicherheit im Luftverkehr," DGLR Jahrestagung 2004, Dresden, Germany

[10] ICAO, "Annex 10 - Aeronautical Telecommunications, Volume 1", 6th Edition, Montreal, 2006

[11] ICAO, "Manual on the Use of the Collision Risk Model (CRM) for ILS Operations, DOC 9274- AN/904", 1st Edition, Montreal, 1980

[12] ICAO, „Airport Services Manual, Part 6 – Control of Obstacles, DOC 9137", 2nd Edition, Montreal, 1983

[13] ICAO, "Annex 14 – Aerodromes, Volume I, Aerodromes Design and Operations", 5th Edition, Montreal, July 2009